Journal of Inorganic Biochemistry 197 (2019) 110702

Contents lists available at ScienceDirect

Journal of Inorganic Biochemistry

journal homepage: www.elsevier.com/locate/jinorgbio

Copper(II) complexes of coumarin-derived Schiff base ligands: Pro- or antioxidant activity in MCF-7 cells?

Louise MacLean[a], Dariusz Karcz[b], Hollie Jenkins[a], Siobhán McClean[c], Michael Devereux[d], Orla Howe[d], Marcos D. Pereira[e], Nóra V. May[f], Éva A. Enyedy[g], Bernadette S. Creaven[a,*]

[a] Centre of Applied Science and Health, TU Dublin - Tallaght Campus, Tallaght D24 FKT9, Ireland
[b] Department of Analytical Chemistry (C1), Faculty of Chemical Engineering and Technology, Cracow University of Technology, Warszawska 24, 31-155 Krakow, Poland
[c] School of Biomolecular and Biomedical Science, University College Dublin, Belfield Dublin 4, Ireland
[d] The Inorganic Pharmaceutical and Biomimetic Research Centre, Focas Research Institute, TU Dublin - City Campus, Kevin St Dublin 8, Ireland
[e] Laboratório de Citotoxicidade e Genotoxicidade, Departamento de Bioquímica, Instituto de Química, Universidade Federal do Rio de Janeiro, Brazil
[f] Research Centre for Natural Sciences, Hungarian Academy of Sciences, Magyar tudósok körútja 2, H-1117 Budapest, Hungary
[g] Department of Inorganic and Analytical Chemistry, University of Szeged, Dóm tér 7, H-6720 Szeged, Hungary

ARTICLE INFO

Keywords:
Copper complexes
Schiff bases
ROS
Speciation

ABSTRACT

A series of copper(II) complexes of Schiff base-derived ligands (**1–7**) were studied for their pro- and antioxidant behaviour in the MCF-7 human breast cancer cell line. The coordination modes of two of the copper(II) complexes were investigated by pH-potentiometry, EPR and UV–Vis spectroscopic methods. The solution studies indicated that monomeric species are present in the Cu(II) – **L1** system at neutral pH, whereas dinuclear species were observed in the case of the Cu(II) – **L7** system. This difference in speciation was reflected in their relative cytotoxicities with the copper(II) complex of **L1**, showing significant cytotoxicity against MCF-7 cells whilst the complex of **L7** was inactive. In fact, only three of the seven complexes studied in this series were cytotoxic to MCF-7 cells but this cytotoxicity did not correlate with their ability to bind to DNA, cleave DNA or act as a pro-oxidant. In contrast to previous copper(II) complexes studied by our group, the compounds studied here do not appear to lead to intracellular reactive oxygen species generation at any significant level. In a yeast-based assay, all of the copper complexes had the ability to protect *Saccharomyces cerevisiae* against menadione-induced oxidative stress but not hydrogen peroxide-induced stress, indicating a lack of catalase activity. Given that the adaptive mechanisms induced by hypoxia in cancer cells have selective effects, with a fine-tuned protection against damage and stress of many kinds, particularly against oxidative stress, chemotherapeutic compounds which are not pro-oxidants may offer a therapeutic advantage.

1. Introduction

Living organisms display complex defence mechanisms to protect against endogenous reactive oxygen species (ROS), based on antioxidants, enzymes and compounds which, in low concentrations dismutate or scavenge ROS. This antioxidant system prevents oxidative damage to cell organelles, plasma membranes, nuclear and mitochondrial DNA, and maintains homeostatic balance [1,2]. However, uncontrolled generation of ROS as well as reactive nitrogen species (RNS) have been implicated in many diseases including cardiovascular disease [3], arthritis [4], neurodegenerative disease [5] and cancer [6]. With respect to cancer, ROS have been shown to be present at high concentrations in some types of cancers, due to the high metabolic activity of the cells [7]. ROS can cause modification of base pairs through abstraction or addition of hydrogen, induction of DNA strand breaks and DNA cross-linking causing DNA mutagenesis and initiating uncontrolled division, the initial step in tumour development [6]. However, numerous studies have also concluded that increasing ROS levels can promote oxidative stress-induced cancer cell death [8]. Thus while the role of ROS in the prevention/induction of cancer is a topic of intense debate in general, the idea of using therapies which *selectively* generate oxidative stress in cancer cells was proposed as a possible therapeutic treatment for malignant cancers [9]. Treatments which depend on the generation of ROS within the cancer cells for their cytotoxic effects are naturally a cause of general concern given the established links between promotion of carcinogenesis and ROS [10]. Nevertheless a number of clinically used chemotherapeutics such as paclitaxel, vinca alkaloids and antifolates are thought to cause cell

* Corresponding author.
E-mail address: bernie.creaven@ittdublin.ie (B.S. Creaven).

https://doi.org/10.1016/j.jinorgbio.2019.110702
Received 15 November 2018; Received in revised form 29 April 2019; Accepted 1 May 2019
Available online 05 May 2019

death through the release of cytochrome *c* and also disruption of the mitochondrial electron transport chain leading to increases in intracellular ROS [11–13]. Procarbazine, which is approved for the treatment of lymphoma and primary brain tumours, also acts by increasing ROS within tumour cells [14].

A series of metal-based compounds, specifically copper(II) complexes of 1,10-phenanthroline, have been proposed as possible alternatives to the widely used metallodrug, cisplatin [15]. These complexes have the ability to generate ROS in the presence of oxygen, and the resultant ROS have been shown to cause random cleavage in DNA at the point where the complex is intercalated with DNA. More recently, other metal-based drugs have been the focus of clinical trials including a series of copper complexes known as the "Casiopeina" series which appear to initiate their anticancer effect through a ROS mechanism [16]. Other copper(II) complexes studied to date as possible chemotherapeutic agents are avid intercalators of DNA and also act as chemical nucleases, with their ability to act as nucleases attributed to their redox activity within the cancer cell [16–18]. A large number of these complexes have a square planar N,N′-O,O′ or N,N′-N,N′ coordination geometry around the metal centre as do the "Casiopeina" series. We and others have identified copper complexes which have shown considerable cytotoxicity against a number of mammalian derived cancer cells lines including human ovarian cancer cells (SKOV-3), breast cancer cells (MCF-7), prostate cancer cells (DU145) and colon adenocarcinoma cell line (HT29) [19–23]. Their solid-state structures indicate that the majority possess square planar geometry around the copper(II) centre. In some cases their anticancer activity has been related to their ability to act as chemical nucleases through the generation of ROS. Conversely, a number of commercial preparations of copper complexes, namely the veterinary Cu(II) complexes of indomethacin which is widely used as an anti-inflammatory treatment in mammals, are thought to exert their affects through their ability to regulate oxidative stress and reduce inflammation [24]. In addition, copper(II) complexes of clinically used non-steroidal anti-inflammatory drugs (NSAIDs) are often more potent anti-inflammatory agents than either the parent NSAID drug or the uncomplexed copper salt [25,26]. Thus the role of copper complexes, in both the generation of and amelioration of, ROS has been established in a number of models and studies.

One series of complexes studied by us, coumarin-derived Schiff bases and their copper(II) complexes (Fig. 1), were cytotoxic to the breast cancer derived MCF-7 mammalian cell line, at concentrations which were comparable to the cytotoxic activity of the commercially used drug, mitoxantrone [27]. That study and other related work on cytotoxic copper complexes with square planar coordination geometry prompted us to look at the mechanism of action of coumarin-derived Schiff bases and their copper(II) complexes in that cell line. Complexes 2–6 shown in Fig. 1, have a N,O-N′,O′ coordination geometry about the copper(II) centre in the solid state but our previous studies had shown that in solution at neutral pH, the predominating Cu(II) species formed in solution equilibrium systems by some of the Schiff base ligands were largely monomeric with coordination of the ligands through the N and the phenolate O^- [27]. The free coordination sites are occupied by solvent molecules at low pH, while in neutral and alkaline solution, mixed hydroxido complexes are formed. The stabilities and coordination modes of the corresponding Cu(II) complexes of various Schiff base ligands did not differ significantly, with one exception, the copper(II) complex formed with **L4**. In this case the ligand has an additional OH group which was found to occupy the third equatorial site of the metal ion of another monomeric unit, and vice versa, forming a highly stable dimeric complex in the acidic pH region. At nearly neutral pH, these bridging OH groups of the dimer are deprotonated. In alkaline solution, the binuclear species are replaced by a mixed hydroxido complex with catecholate coordination, which is also significantly more stable than the other mixed hydroxido complexes with Schiff-base binding mode for the other ligands. The poor aqueous solubility of the other ligands and complexes hindered their full investigation so a more water soluble ligand **L7** and complex were synthesised and their solution behaviour at physiological pH investigated. The pro- or antioxidant nature of the complexes was also examined in this study, together with the nature of their interaction with DNA.

2. Results and discussion

2.1. Synthesis of Schiff base complexes

The structures of the ligands and complexes used in this study are given in Fig. 1. The synthesis and characterisation of the ligands **L1**-**L6** and complexes **2–6** have been previously reported [27,28]. **L4** had the greatest solubility in a range of solvents and also had displayed a different coordination mode at physiological pH to the other Schiff bases in our previous study and thus a trihydroxy Schiff base, **L7**, was synthesised and its Cu(II) complex isolated. The ligands were prepared in two steps, firstly through the synthesis of a coumarin-based compound 7-amino-4-methylcoumarin via a Pechmann condensation reaction between an aromatic phenol, 3-aminophenol, and a β-keto ester, ethyl acetoacetate. 7-amino-4-methylcoumarin was then reacted with various substituted aldehydes to generate a series of Schiff bases, **L1**-**L7**, (Scheme 1). Complex **1** had not been isolated in pure form in our previous studies but was successfully isolated for these studies and included here. Details of the synthesis and analytical data are given in Supplementary Information. We were unable to isolate crystals of the complexes, though a related complex previously reported by our group, showed a mononuclear Cu(II) centre bound to two Schiff base ligands in a distorted square planar coordination environment around the metal centre [28]. Table 1 compares the ligand IR bands to the bands of the corresponding complexes for complexes **1** and **7**. For complex **7** the

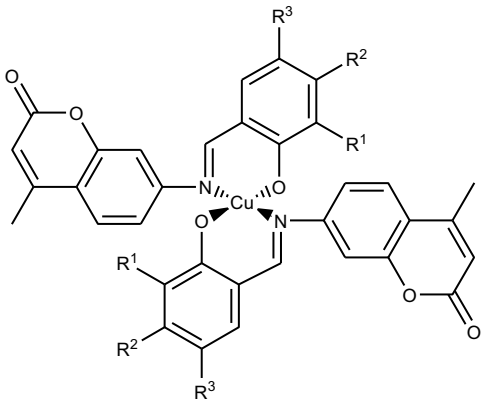

Complex	R^1	R^2	R^3
1	OCH_2CH_3	H	H
2	H	H	NO_2
3	OCH_3	H	NO_2
4	OH	H	H
5	OCH_3	H	H
6	I	H	I
7	OH	OH	H

Fig. 1. Proposed solid state structure of copper(II) complexes of coumarin-derived Schiff base ligands.

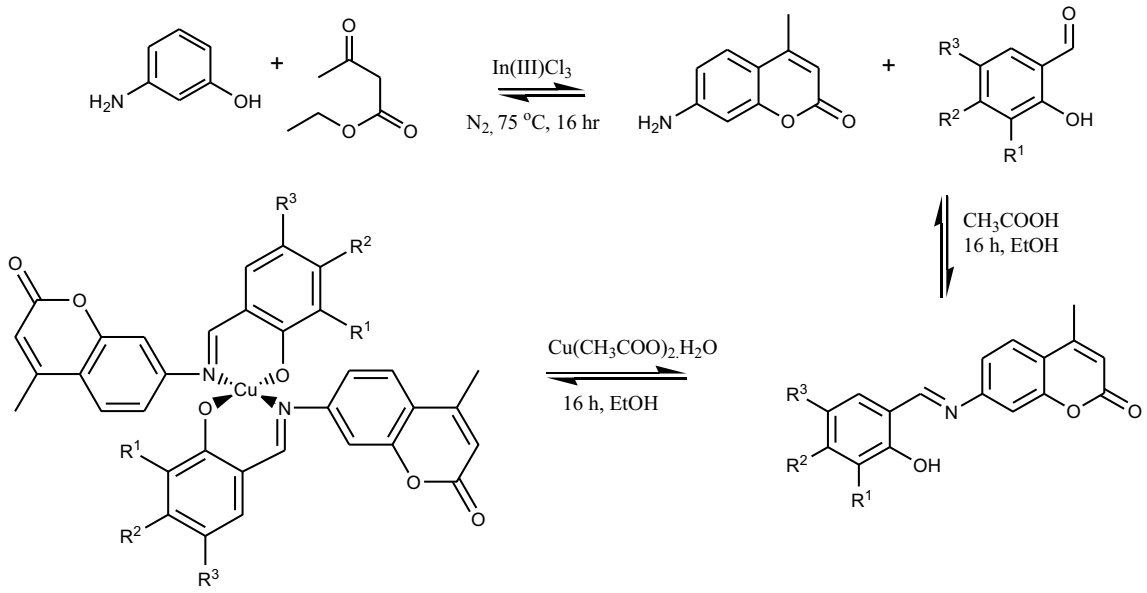

Scheme 1. General synthetic scheme for coumarin-derived Schiff bases ligands and their copper complexes (substituents R^1, R^2 and R^3 given in Fig. 1).

imine stretch vibration 1639 cm^{-1} in the free ligand was observed at a slightly higher frequency in the Cu(II) complex at 1643 cm^{-1}, indicating coordination of the Schiff base ligands may be via the imine nitrogen. The ν_{C-O} values for the complexes undergo a blue shift in the complex, from 1296 cm^{-1} to 1312 cm^{-1}, implying coordination via the hydroxylato O of the Schiff base ligands. However, the imine band at 1624 cm^{-1} in **L1** was unresolved from the C=C carbon band upon complexation. A band at 1296 cm^{-1} shifted to 1312 cm^{-1} upon complexation and was assigned to ν_{C-O} stretch of the phenolate group. The close similarity of the latter IR bands to those of the complexes previously isolated and to the complex characterised by X-ray crystallography, indicated that the structure in the solid state of the complex **1** is likely to have a distorted square planar N,O-N′,O′ coordination mode to the copper(II) centre. The solid state structure of complex 7 is likely to be polymeric in nature with binding to both catecholate and imine moieties in the structure.

2.2. Proton dissociation processes and fluorescence of the studied ligands (L1, L7)

A series of Schiff base-derived coumarin ligands were previously studied including **L1**, **L4** and **L5** (Fig. 1) [27], but solubility issues had prevented the study of the other Cu(II)–ligand systems. The pK_a value of **L1**, which contains an ethoxy group in the R^1 position, was re-determined with additional experimentation and is in good agreement with the published data. Additional EPR data for **L1** were recorded for this work to confirm the data from previous studies. **L7** possesses two additional hydroxyl groups at R^1 and R^2 positions compared to the core molecule. Due to the insufficient water solubility of the ligands the studies were performed in an 80% (v/v) dimethyl sulfoxide (DMSO)/H_2O solvent mixture. pK_a values of these ligands have been determined by pH-potentiometry and UV–visible (UV–vis) spectrophotometry (Table 2).

Compound **L1** has only one dissociable proton attributed to the OH moiety that can be liberated in the studied pH range (2–14.5), while **L7** has two additional pK_a values due to the presence of the two extra hydroxyl groups. Both ligands display intense absorption bands in the UV–vis region due to the extended conjugated electronic system of the imine and coumarin moieties (representative spectra are shown for **L7** in Fig. 2a). Deprotonation of the phenolic OH groups results in characteristic spectral changes, namely the development of a strong band at the 400–470 nm range. The second and third deprotonation steps of **L7** are strongly overlapping at high pH, thus a pK_a value could be determined only for the first deprotonation process via the deconvolution of the spectra up to pH 10.4 (Fig. 2b,c.). Notably, the possible O_2

Table 2
Proton dissociation constants (pK_a) of **L1** and **L7** and overall stability constants (logβ) of their Cu(II) complexes determined by pH-potentiometric titrations in 80% (v/v) DMSO/H_2O. (T = 25 °C; I = 0.1 M (KCl)).

		L1[a]		L7
Model I	pK_a (HL)	9.46 ± 0.03[b]	pK_1 (H_3L)	8.41 ± 0.09[b]
	logβ $[CuL]^+$	6.65 ± 0.09	pK_2 (H_2L^-)	13.51 ± 0.07
	logβ $[CuLH_{-1}]$	−1.34 ± 0.09	pK_3 (HL^{2-})	15.30 ± 0.05
	logβ $[CuLH_{-2}]^-$	−12.1 ± 0.1	logβ $[CuLH_2]^+$	38.6 ± 0.2
	pK_a $[CuL]^+$	7.99	logβ [CuLH]	30.64 ± 0.09
	pK_a $[CuLH_{-1}]$	10.74	logβ $[CuL]^-$	15.8 ± 0.2
			pK_a $[CuLH_2]^+$	7.52
			pK_a [CuLH]	14.87
Model II	logβ $[CuL]^+$	6.61 ± 0.08		
	logβ $[CuLH_{-1}]$	−1.34 ± 0.08	logβ $[Cu_2L_2H_4]^{2+}$	78.7 ± 0.1
	logβ $[Cu_2L_2H_{-4}]^{2-}$	−20.8 ± 0.2	logβ $[Cu_2L_2H_2]$	62.4 ± 0.1

[a] Data published for **L1**: pK_a = 9.28; logβ $[CuL]^+$ = 6.30; logβ $[CuLH_{-1}]$ = −1.71; $[CuLH_{-2}]^-$ = −12.7; pK $[CuL]^+$ = 8.01; pK $[CuH_{-1}]$ = 10.99 in Ref. [27].

[b] **L1**: 9.44 ± 0.08; **L7**: pK_1 (H_3L) = 8.38 ± 0.02 determined by UV–vis titrations.

Table 1
IR bands for coumarin-derived Schiff base ligands and their complexes.

Ligand	ν(CH=N) cm^{-1}	ν(C=O) cm^{-1}	ν(C−O) cm^{-1}	Complex	ν(CH=N) cm^{-1}	ν(C=O) cm^{-1}	ν(C−O) cm^{-1}
L1	1624	1724	1250	1	Unresolved	1728	1219
L7	1639	1705	1296	7	1643	1701	1312

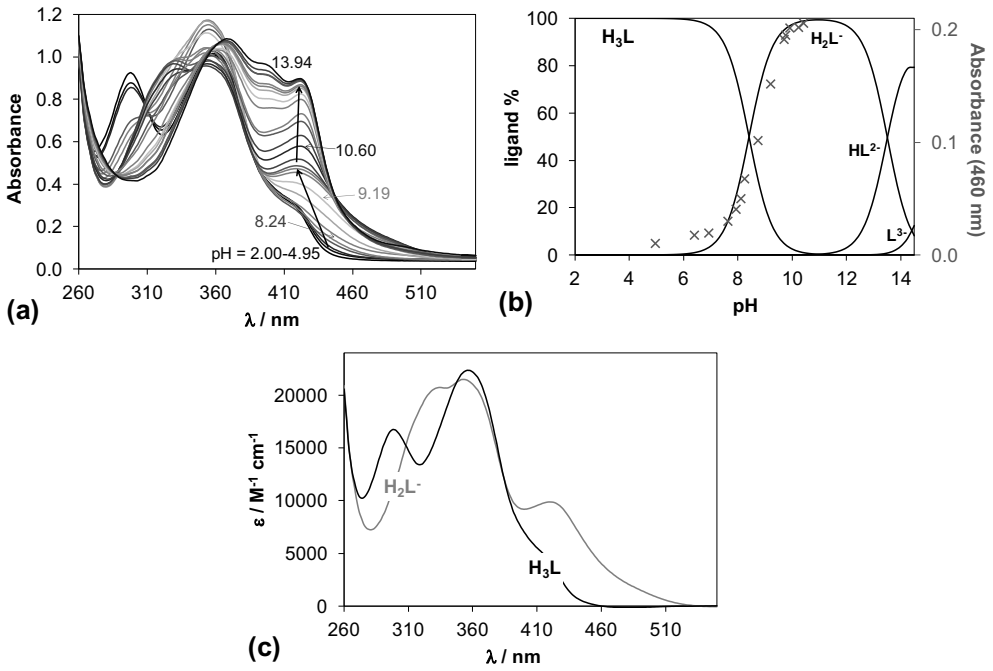

Fig. 2. UV–visible spectra recorded at various pH values for **L7** (a); concentration of distribution curves (solid lines) together with absorbance values at 460 nm up to pH 10.4 (×) (b); calculated molar absorbance spectra of H_3L and H_2L^- species (c). (80% (v/v) DMSO/H_2O; T = 25 °C, I = 0.10 M (KCl); c_L = 48 μM; l = 1 cm).

sensitivity of the pyrogallol moiety of **L7** makes the pH-potentiometric results more reliable compared to UV–Vis.

The pK_a of the core molecule (R^1, R^2 = –H) is somewhat higher (9.66) [27] than the pK_1 values of **L1** and **L7** due to the presence of the ethoxy and especially the hydroxyl groups, respectively. pK_2 and pK_3 values of **L7** are fairly high, most probably as a result of the formation of strong hydrogen bond between the phenolate O^- and the adjacent OH group. Compounds **L1** and **L7** exhibit strong fluorescence similarly to the analogous compounds [27]. However, the emission intensities seem to be dependent on the substituents as **L7** is not as fluorescent as **L1** (Fig. 3).

2.3. Complex formation with Cu(II) ions

Complex formation processes of **L1** and **L7** with Cu(II) ions were also studied by the combined use of pH-potentiometry and EPR spectroscopy in a 80% (v/v) DMSO/H_2O solvent mixture. Representative titration curves are shown for the Cu(II) – **L7** system in Fig. 4. Although stability constants for the Cu(II) complexes of **L1** were determined by pH-potentiometry in our former work [27], measurements were repeated and completed by the EPR titrations. The overall stability

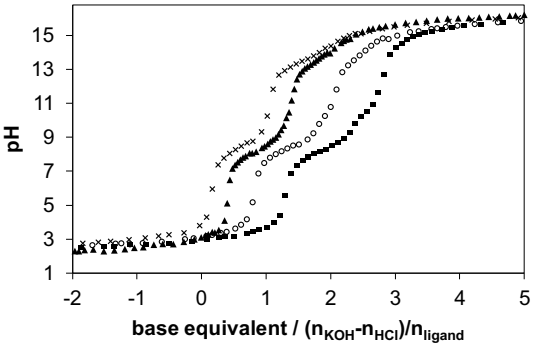

Fig. 4. pH-potentiometric titration curves recorded for the Cu(II) – **L7** system: ligand alone (×); Cu:**L7** = 1:3 (▲), 1:2 (○), 1:1 (■). (80% (v/v) DMSO/H_2O; T = 25 °C, I = 0.10 M (KCl)).

constants (logβ) and pK_a values of the Cu(II)-ligand systems obtained by pH-potentiometry which give the best fit to the experimental data are listed in Table 2. The titration curves suggest the formation of a large amount of mixed hydroxido complexes in basic solution with **L1**,

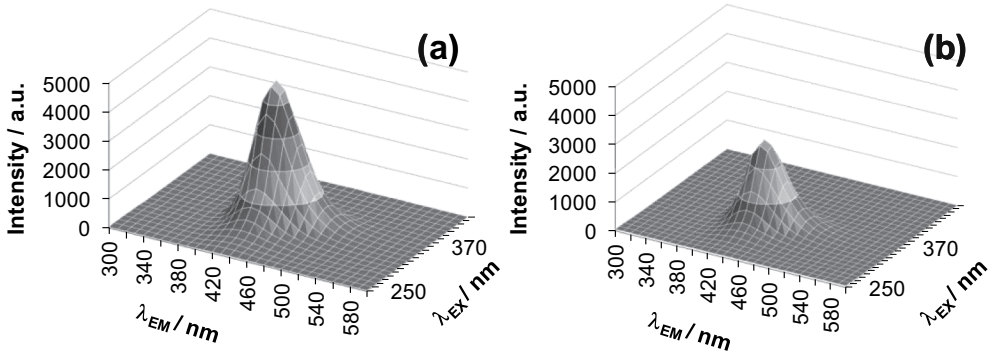

Fig. 3. 3D-fluorescence spectrum of **L1** (a) and **L7** (b) at neutral pH (9.35) in 80% (v/v) DMSO/H_2O under the same condition (T = 25 °C, I = 0.10 M (KCl); c_L = 1 μM; l = 1 cm).

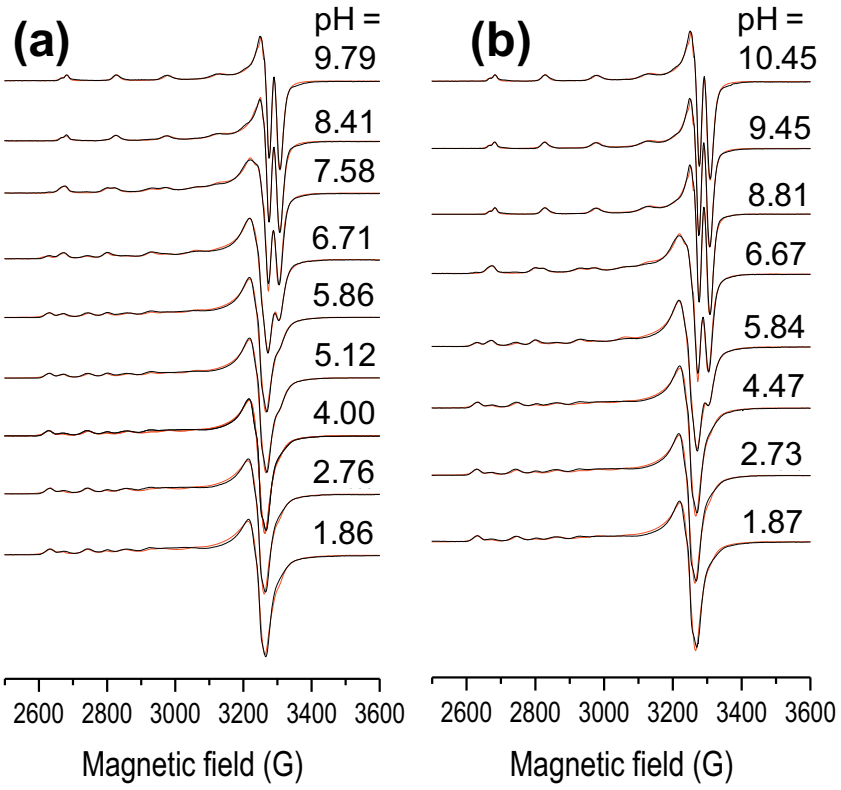

Fig. 5. EPR spectra recorded at various pH values for the Cu(II) – **L1** system at 1:1 (a) and 1:3 (b) metal-to-ligand ratio (black lines) together with the simulated spectra (red lines). (80% (v/v) DMSO/H_2O; T = 77 K, I = 0.10 M (KCl); $c_{Cu(II)}$ = 1 mM (a), 0.67 mM (b)).

therefore $[CuLH_{-1}]$ and $[CuLH_{-2}]^-$ are considered as [CuL(OH)] and $[CuL(OH)_2]^-$ species. However, formation of mixed hydroxido complexes is also probable in the case of **L7**, but deprotonation of a coordinated water molecule or the further hydroxyl groups at positions R^1 and R^2 cannot be distinguished on the basis of pH-potentiometric titrations. It should be noted that only the formation constants for complexes in which the metal-to-ligand ratio is 1:1 could be calculated.

In order to confirm the speciation model obtained by the pH-potentiometric measurements, and to elucidate the coordination modes, EPR spectroscopy was applied at room temperature and at 77 K. A pH-dependent series of experimental and simulated frozen solution EPR spectra for the Cu(II) – **L1** system are depicted in Fig. 5, and EPR spectroscopic data obtained from the simulation are given in Table 3. The slow rotation of the complexes resulted in broad room temperature spectra which were not simulated (Fig. S4.1). It is noteworthy that there was no indication of the formation of any *bis*-ligand complexes even at higher ligand excess under the conditions used here. The intensity of the EPR signal significantly decreased at pH > 11 in the pH-range of the formation of the $[CuL(OH)_2]^-$ species as the concentration distribution curves shown in Fig. 6 and which are denoted by black lines.

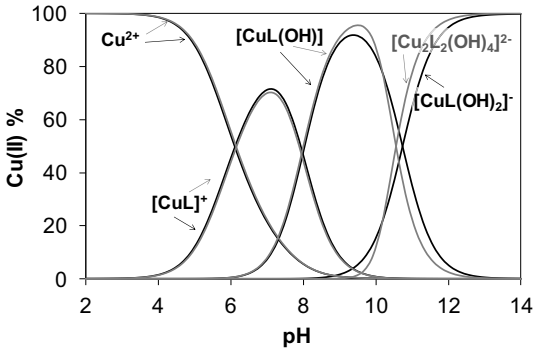

Fig. 6. Concentration of distribution curves of the Cu(II) – **L1** system on the basis of the determined stability constants using pH-potentiometry (model I: black lines, model II: grey lines). (80% (v/v) DMSO/H_2O; T = 25 °C, I = 0.10 M (KCl); $c_{Cu(II)} = c_L$ = 1 mM).

Table 3
EPR parameters at 77 K for the Cu(II) complexes of **L1** in 80% (v/v) DMSO/H_2O.[a]

	g_x,	g_y	g_z	A_x/G	A_y/G	A_z/G	a_x^N/G a_y^N/G a_z^N/G	$g_{o,calc}$[b]
Cu^{2+}	2.0787(1)	2.0787(1)	2.4060(3)	1.5(5)		113.7(2)		2.1878
$[CuL]^+$	2.0836(1)	2.0555(1)	2.3559(3)	10.0(1)	14.9(1)	127.2(3)		2.1650
[CuL(OH)]	2.0649(1)	2.0617(2)	2.3242(3)	0.0(3)	14.2(1)	147.5(2)	4.7	2.1503
							9.7	
							9.9	
$[Cu_2L_2(OH)_4]^{2-}$	Inactive							

[a] The confidence intervals of the parameters regarding the last digit are given in parentheses. The hyperfine coupling constants and the relaxation parameters are given in G (10^{-4} T) units, and refer to the isotope 63Cu.
[b] Calculated isotropic values via the equation $g_o = (g_x + g_y + g_z)/3$.

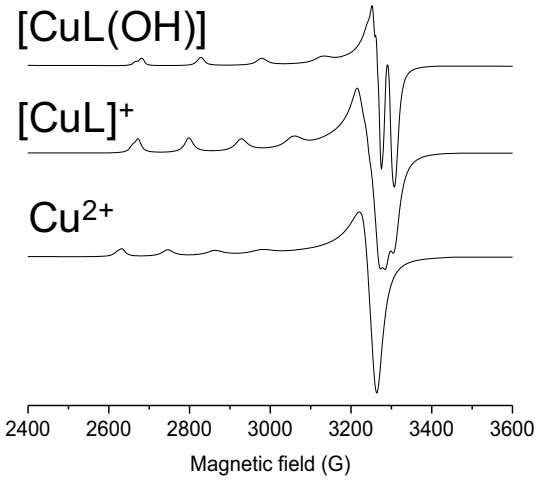

Fig. 7. Calculated component EPR spectra obtained for species formed in the Cu(II) – **L1** system. (80% (v/v) DMSO/H_2O; T = 77 K, I = 0.10 M (KCl)).

This phenomenon indicated that the $[CuL(OH)_2]^-$ species is most probably a dimeric species, with composition $[Cu_2L_2(OH)_4]^{2-}$ as exchange interaction of close copper ions results in the disappearance of the EPR signal. Therefore the pH-potentiometric data were re-evaluated by incorporating the latter dimeric species into the speciation model.

The stability constants (in model II) are collected in Table 2, and new concentration distribution curves were computed (in Fig. 6, with grey lines). Simulated anisotropic EPR spectra for Cu(II), $[CuL]^+$ and [CuL(OH)] are shown in Fig. 7. These spectra and the determined EPR parameters (Table 3) for the Cu(II) – **L1** complexes are fairly similar to those of the core compound (R^1, R^2 = –H) suggesting similar coordination modes. Thus in $[CuL]^+$ the coordination of the phenolate oxygen and the Schiff-base nitrogen is very feasible (though nitrogen splitting is not resolved), [CuL(OH)] contains a hydroxido ligand in addition, for which one nitrogen splitting was taken into account, while $[Cu_2L_2(OH)_4]^{2-}$ is a hydroxido bridged EPR-silent $[(CuL(OH))_2(\mu\text{-}OH)_2]^{2-}$ species.

In the case of the Cu(II) – **L7** system room temperature spectra were recorded. However, EPR spectroscopy could not be used as from pH 4–15 the signal intensity decreased completely (Fig. S4.2). The samples were back-acidified and the signal of the free Cu(II) ions were regained suggesting that no reduction of Cu(II) took place in the basic pH range. This indicates the formation of dimeric or oligomeric complexes. We propose that the OH group on the R^1 position is able to bind to another copper complex and vice versa forming an EPR-silent dimer species. Therefore the pH-potentiometric data were fitted with the assumption of the formation of dimeric complexes in solution as well and data are shown in Table 2 (model II). Using the stability constants obtained from both models, distribution curves were calculated for the Cu(II) – **L7** system (Fig. 8).

Based on the calculations we can conclude that complexes $[CuL]^+$ and [CuL(OH)] are present in the Cu(II) – **L1** system at neutral pH, while at the same pH $[Cu_2L_2H_2]^{2+}$ and $[Cu_2L_2H_2]$ species exist in the case of Cu(II) – **L7**. In the latter two complexes the protons can be attributed to the ligand's non-coordinating phenolic OH groups. Formation of *bis* complexes was not observed in solution. The complex formation starts at much lower pH values with **L7** indicating the higher stability of the Cu(II) – **L7** complex relative to the Cu(II) – **L1** system. Given that the dominant species in solution at neutral pH seem to be quite different for the two complexes, with the coordination of **L1** to Cu (II) ions similar to the previously studied coumarin-derived Schiff bases and **L7** coordination to Cu(II) ions similar to the previously studied **L4**, it would be interesting to compare their relative bioactivities to each other and to that of all of the previously synthesised complexes.

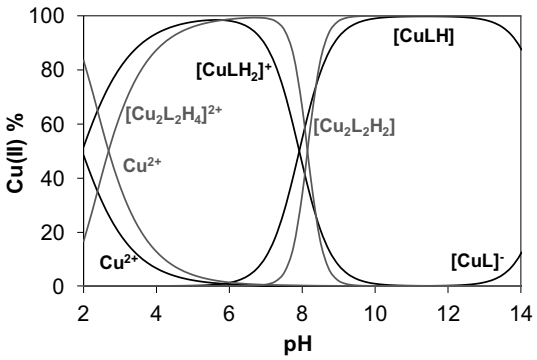

Fig. 8. Concentration of distribution curves of the Cu(II) – **L7** system on the basis of the determined stability constants using pH-potentiometry (model I: black lines, model II: grey lines). (80% (v/v) DMSO/H_2O; T = 25 °C, I = 0.10 M (KCl); $c_{Cu(II)} = c_L$ = 1 mM).

2.4. Cytotoxicity studies

Previous studies on coumarin derivatives and their Cu(II) complexes isolated by our group have shown considerable anticancer activity against a number of cell lines [20,28,29]. The cytotoxicity of ligands **L1**-**L6** and complexes **2–6** was previously assessed against MCF-7 human breast cancer cells using methylthiazolyldiphenyltetrazolium bromide-based assay (MTT) [20] (Table 4) and for comparison are presented here with the new data. The most cytotoxic compounds were complexes **3** and **6** showing IC_{50} values of 34.5 ± 6.0 μM and 79.8 ± 5.0 μM respectively. The positive control used in this study was mitoxantrone, approved for use in the treatment of metastatic breast cancer and to which MCF-7 cell lines are sensitive [30]. The enhanced solubility of complex **7** did not result in a more cytotoxic compound but the cytotoxicity of complex **1** was comparable to mitoxantrone. Solution studies had shown that upon dissolution of the complexes it's likely in all cases that either monomeric or dimeric species are formed, therefore a stoichiometric amount of free ligand is also present in all solutions tested. Hence, the free ligands and the free copper salt were assayed in all studies carried out here. None of the ligands, including **L1** and **L7**, or the free copper salt were cytotoxic to MCF-7 cells.

2.5. Determination of SOD and CAT mimetic ability in a cell-free system

The generation of hydroxyl radicals through the ability of the complexes to dismutate superoxide to hydrogen peroxide, which can then undergo Fenton chemistry to generate highly reactive hydroxyl radical has been proposed to be intimately linked to the subsequent DNA damage resulting in cell death. The most widely used method of

Table 4
Summary of IC_{50} values of complexes **1–7** (μM) measured after 24 h against MCF-7 breast cancer cell line. Values calculated from 3 independent experiments.

Series	Ref	Complex	IC_{50} values (μM ± SEM)
Schiff base complexes		**1**	69.3 ± 7.6
	20	**2**	> 100[a]
	20	**3**	34.5 ± 6.1[a]
	20	**4**	> 100[a]
	20	**5**	> 100[a]
	20	**6**	79.8 ± 4.6[a]
		6	63.8 ± 4.6
		7	> 100
Drug	20	Mitoxantrone	15.0 ± 8.7[a]
	20	Doxorubicin	71.6 ± 1.5[a]
Ctrl	3, 25,20	$CuSO_4$	> 100[a]

[a] IC_{50} values from reference [20]. These values were measured in the same laboratory as those reported for the current work using the same cell line.

Table 5
Coumarin-derived Schiff base complexes and their in vitro SOD and CAT activities. SOD activity are expressed as an IC_{50} (μM), which is the concentration of complex required to inhibit 50% of the blue formazan formation. CAT activity was measured via the volume of oxygen evolved from a reaction vessel containing 10 cm^3 of 35% aqueous H_2O_2 in the presence of 10 mg of complex and 50 mg of imidazole base.

Complex no.	R^1	R^2	R^3	SOD activity IC_{50} ± 0.5 (μM)	CAT activity volume of O_2 evolved (mL/min)
1	OCH_2CH_3	H	H	–	–
2	H	H	NO_2	1.15	13.5
3	OCH_3	H	NO_2	0.99	23.9
4	OH	H	H	1.39	7.9
5	OCH_3	H	H	1.08	4.7
6	I	H	I	0.85	Inactive
7	OH	OH	H	–	–
Veterinary drug $[Cu_2(indo)_4(H_2O)_2]$				1.31	

determining the superoxide dismutase (SOD) activity of a compound is via a nitro blue tetrazolium (NBT) assay which utilises xanthine–xanthine oxidase as a superoxide generator [19,31]. Initially complexes **2–6** and ligands **L2-L6** were tested for their ability to inhibit the reduction of NBT to blue formazan by scavenging superoxide radicals, which were generated by xanthine oxidase during the conversion of xanthine to urate. Whilst none of the ligands showed any SOD activity, all of the tested complexes did (Table 5). The complexes had a much lower catalytic efficiency than native CuZn-SOD, which has an IC_{50} value of 0.04 μM [32], and nearly all of these complexes exceeded the SOD activity of the marketed veterinary drug, $[Cu_2(indomethacin)_4(H_2O)_2]$, a dinuclear copper complex which has an IC_{50} value of 1.31 μM [32].

The SOD-mediated dismutation of $O_2^{\cdot-}$ species generates H_2O_2, which in turn may undergo catalase-mediated decomposition to H_2O and O_2. A study of Fe(III), Cu(II) and Mn(II) complexes containing the (N,N,N,O) donor ligand 1-[bis(pyridine-2-ylmethyl)amino]-3-chloropropan-2-ol (HPCINOL) showed that all three complexes behaved as SOD and CAT mimics and the Fe(III) complex exhibited the highest protective effect, followed by Cu(II) and Mn(II) [33]. In terms of the complexes acting as DNA nucleases, their ability to disproportionate H_2O_2 to oxygen and water, would argue against these complexes being good nucleases. Reasonable catalase activity could only be recorded for complex **3** (Table 5), which was identified as the most cytotoxic compound. At the time of these studies, complex **1** was not available in pure form. Its more recent isolation together with the newly synthesised complex **7** allowed the determination of all of the complexes' antioxidant activity in a yeast-based assay similar to that used to assess the SOD and CAT activity of the copper, manganese and iron complexes mentioned above [33,34].

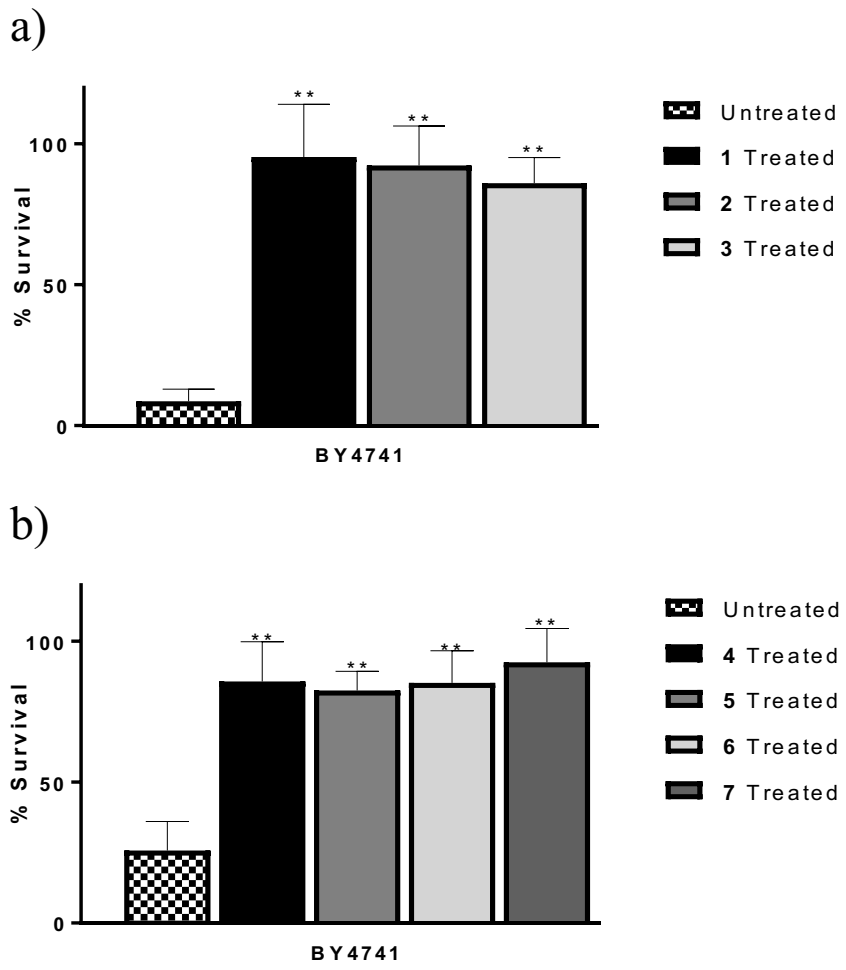

Fig. 9. Effect of biomimetics on the survival rates of *S. cerevisiae* wild type cells exposed to oxidative stress. Cells were preincubated with 100 μM of complex for 2 h (a) complexes **1–3** and (b) **4–7**, and then exposed to 30 mM menadione, a superoxide generator. Cells were cultured in 2% YPD medium and cell viability was measured by plating in triplicate on 2% YPD solid medium and expressed as percentage of survival relative to a negative control. The results represent the mean ± SEM of at least three independent experiments.

2.6. Antioxidant activity of complexes 1–7 in wild type cells

Saccharomyces cerevisiae is a facultative anaerobe, with the ability to respire aerobically and anaerobically in the absence of oxygen. It has an inducible stress response which, similar to mammalian cell systems, activates genes encoded for SOD and CAT enzymes when exposed to superoxide and hydrogen peroxide respectively [21,33,34]. This yeast species has been shown to be a good model for determining the SOD and CAT-like activity of metal-based complexes [33,34].

Wild type cells were grown in glucose rich media to mid-log phase of growth, as at this point, the natural SOD and CAT defences are minimal as they are cultured under fermentative conditions [33–35]. Therefore, any SOD or CAT activity observed will be, as far as possible, the result of the antioxidant capability exhibited by the complex, rather than the yeast cells own ROS defence enzymes. In the positive control, cells were treated with sub-lethal concentrations of menadione or hydrogen peroxide to induce an oxidative response. Test conditions involved cells which were pre-treated with compounds and subsequently treated with stressor to evaluate any potential protective effects of the metal complexes. The viable cell count recorded for the negative control, where cells were allowed to grow freely without stressor or complex pre-treatment, represented 100% survival and the positive control and complex treated cells were calculated as a percentage of this. DMSO, the solvent which was used to dissolve the complexes at a concentration of 14 mM, was also tested and showed no ability to protect against stress in either wild type cells or either of the mutant cells strains (Supplementary Information).

All Schiff base complexes **1–7** showed statistically significant SOD activity in the wild type studies ($P < 0.001$) at 100 μM of complex relative to the positive control, Fig. 9a) and b). Surprisingly, given the results presented in Table 5 above, none of the complexes **1–7**, Fig. 10a), b) and c), showed ability to protect cells against hydrogen peroxide-induced stress. The Schiff base ligands and copper salts demonstrated no ability to protect the cells against menadione-induced superoxide stress or hydrogen peroxide-induced stress, indicating that they are neither SOD nor CAT mimics (Supplementary Information).

As the complexes had only shown SOD activity in the wild type cell studies, three of the complexes, **4–6**, were studied to monitor if the complexes could demonstrate SOD activity in the SOD mutant model. As the mutants are more sensitive to oxidative stress due to diminished defences **[**33,34**]**, a lower concentration of stressor was used to treat the mutant cells compared to the wild type cells, but all other conditions in the individual assays remained the same. The antioxidant activity of DMSO was also tested as the vehicle control. All three complexes showed statistically significant ability to protect the *sod1*Δ mutant cells from menadione-induced oxidative stress, ($P = 0.0073$, 0.0406, 0.0080 for **4**, **5** and **6** respectively) (Fig. 11).

2.7. ROS activity: measurement of intracellular oxidative stress

The fluorescent probe 2′,7′-dichlorodihydrofluorescein diacetate, (H_2DCFDA), was utilized in detecting ROS produced by these complexes in MCF-7 cells, where H_2DCFDA is oxidised to fluorescent 2′,7′-dichlorofluorescein (DCF) in the presence of oxidants. Results are then expressed as increases in cellular ROS levels after exposure to test compound relative to fluorescence levels in untreated cells and compared to a solvent control and the positive control, tert-butyl hydroperoxide (TBHP). TBHP, is an organic source of hydrogen peroxide, and is used at a concentration of 0.5 μM to induce oxidative stress in MCF-7 cells.

L1-**L7** showed no discernible ability to induce ROS generation in MCF-7 cells (Supplementary Information) and five of the seven Schiff base-derived complexes, **1**, and **4–7**, had the ability to exhibit concentration dependent ROS generation in MCF-7 cells but only at relatively high concentration with one exception, complex **1** (Fig. 12). Complex **1** induced ROS at the lower concentration of 12.5 μM and upwards at 180 min. Complexes **4** and **7** had the least ability, with ROS induction only apparent after 180 min at 50 and 100 μM concentrations. None of the Schiff base-derived complexes induced ROS at < 120 min of incubation, with complexes **5** and **6** inducing ROS at 100 μM after 120 min. ROS generation is a well-established feature of copper(II) complexes and many such complexes generate considerable ROS at shorter timescales and at much lower concentrations than the complexes assessed here [19,23,38–40].

2.8. DNA binding properties

The yeast-based assays described above identified that all of the complexes had SOD mimetic activity but no catalase mimetic ability and therefore the reaction of the complexes with superoxide may lead to the generation of increased levels of hydrogen peroxide in the cell. Given the ubiquitous presence of catalytic amounts of Fe(II) in living systems, hydrogen peroxide could then react via Fenton chemistry to generate hydroxyl radicals. As copper complexes are thought to most likely initiate their cytotoxic effect through oxygen-dependent or -independent DNA cleavage after intercalation with DNA, the DNA binding properties of the complexes were investigated. The most well-known types of copper complex-based nucleases are those incorporating 1,10-phenanthroline (phen) such as $[Cu(phen)_2]^{2+}$ and copper(II) complexes of (N,N,O,O) ligands [19,23,38–40]. The ability of the ligands and complexes to bind to DNA was assessed using a competitive ethidium bromide (Et^+) fluorescence displacement assay using CT-DNA (calf-thymus, ultrahigh purity) which allowed comparison with the known DNA intercalator actinomycin D and the DNA minor groove binder pentamidine [36,37]. None of the ligands showed any ability to interact with DNA and only complexes **6** and **7** showed reasonable ability to interact, though not as avidly as actinomycin D, (Table 6), (full data given in Supplementary Information) or indeed to related copper(II) square planar complexes previously published.

2.9. DNA nuclease ability

The ability of a complex to bind to DNA is not always followed by the ability to have nuclease activity and therefore all of the complexes and ligands were also assessed for their ability to cleave DNA. The oxidative DNA cleavage of the ligands and their copper(II) complexes were measured in the presence of added reductant using supercoiled (SC) pBR322 DNA. There was no observed nuclease activity for any of the ligands up to a concentration of 100 μM and indeed even at 100 μM, limited cleavage was noted for a few of the complexes (Supplementary Information). The positive control in the assay was 20 μM $[Cu(phen)_2]_2^{+}$, a complex known to cleave DNA. We have previously reported that copper(II) complexes with square planar coordination geometry have shown DNA nuclease ability similar to that of $[Cu(phen)_2]^{2+}$ [19,39,40]. Thus the lack of nuclease ability of these complex, given the cytotoxicity of complexes **1**, **3** and **6,** was surprising and indicates that the cytotoxicity of these complexes is unlikely to be related to nuclease activity.

3. Conclusions

The pro/antioxidant behaviour of a series of copper(II) complexes of coumarin-derived Schiff bases was studied in order to evaluate their potential as inflammatory modulators to probe the basis of their cytotoxicity in MCF-7 cells. Two of these complexes had shown anticancer activity in previous studies and a further two complexes were added to this study, primarily as the better solubility of their ligands allowed for speciation studies using spectroscopic and potentiometric techniques. Whilst the solid state analytical data for the complexes indicated that the copper ion was likely coordinated to two Schiff base ligands via 2 × (N,O) donor set, the formation of *bis* complexes was not observed in solution. Instead the solution studies indicated that *mono* species

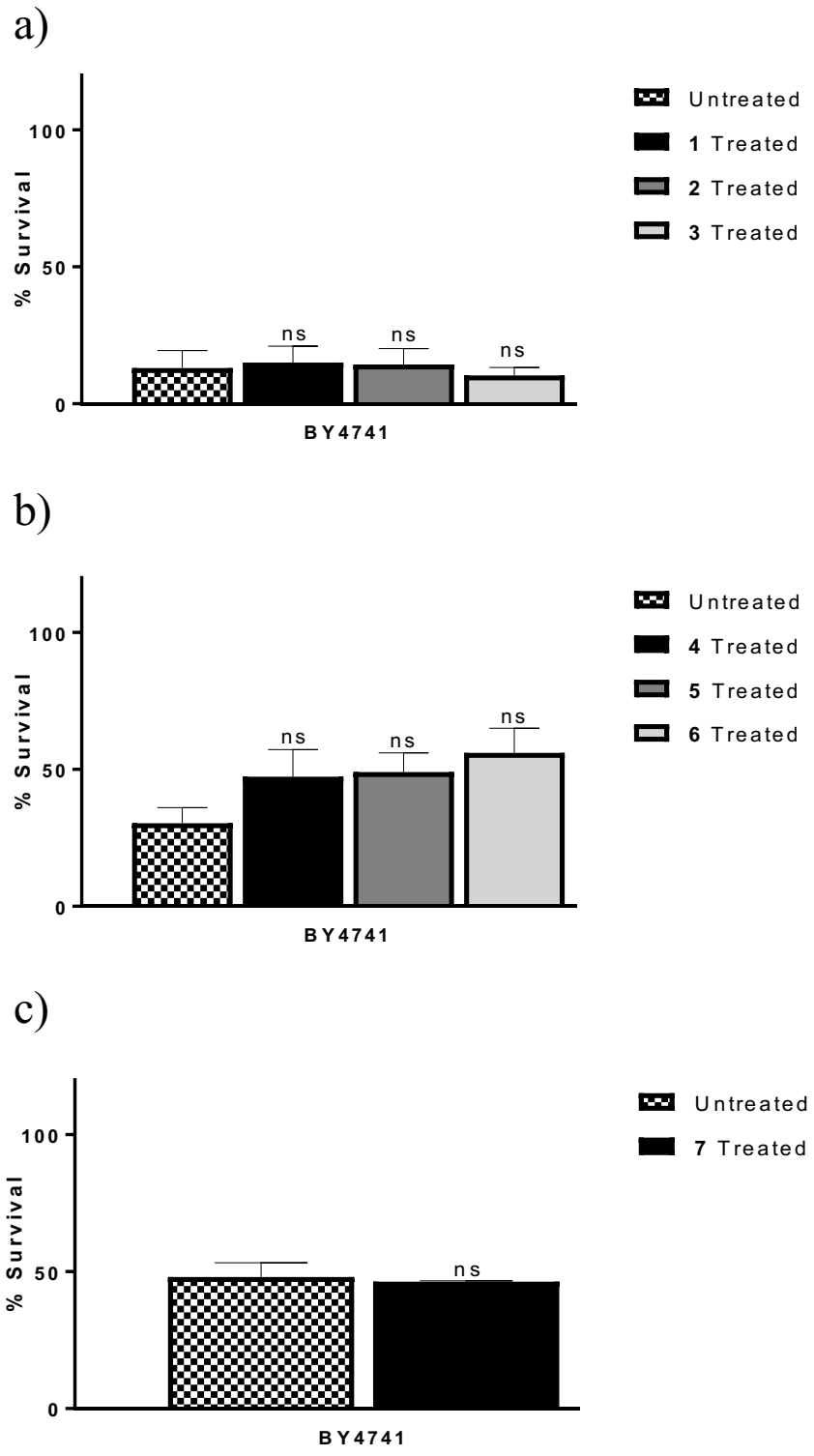

Fig. 10. Effect of the biomimetics on the survival rates of *S. cerevisiae* wild type cells exposed to oxidative stress. Cells were preincubated with 100 μM of complex for 2 h, a) **1–3**, b) **4–6** and c) **7**, and then exposed to 2 mM H_2O_2. Cells were cultured in 2% YPD medium and cell viability was measured with and without exposure to oxidative stress by plating in triplicate on 2% YPD solid medium and expressed as percentage of survival relative to a negative control. The results represent the mean ± SEM of at least three independent experiments.

$[CuL]^+$ and [CuL(OH)] are present in the Cu(II) – **L1** system at neutral pH, similar to the speciation determined for Cu(II) – **L5** system and other related Schiff bases ligands which were measured previously [27]. Dinuclear species $[Cu_2L_2H_2]^{2+}$ and $[Cu_2L_2H_2]$ were observed in the case of ligand **L7,** and previously for **L4** [27]. While for **L1** and **L5**, the Cu(II) was found to bind to the imine nitrogen and phenolic oxygen of the ligand giving an N,O binding mode, Cu(II) - **L4** was suggested to have a O,O binding mode to two neighbouring phenolic oxygens, which may also be the case for Cu(II) – **L7** due to the presence of three neighbouring hydroxyl groups, but due to EPR silence over a wide pH range, the exact binding mode could not be established. Unfortunately the solubility of the other ligands in solution did not allow for the study

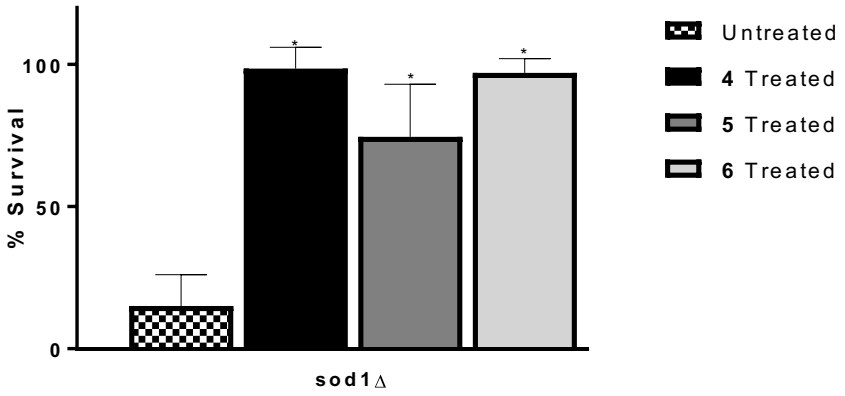

Fig. 11. Effect of the biomimetics on the survival of *S. cerevisiae sod1*Δ mutant cells when exposed to oxidative stress. Cells were preincubated with 100 μM of complexes **4–6** for 2 h and then exposed to 1.2 mM menadione. Cells were cultured in 2% YPD medium and cell viability was measured with and without exposure to oxidative stress by plating in triplicate on 2% YPD solid medium and expressed as percentage of survival relative to a negative control. The results represent the mean ± SEM of at least three independent experiments.

of their speciation. Thus, while the complexes studied here may be similar in structure to other copper-based chemotherapeutics in the solid state, their solution behaviour would suggest that they undergo partial anation or dimerisation at physiological pH, with dimerization likely if O,O binding mode is facilitated by the presence of additional hydroxy groups.

Complex **1** had considerable activity against the MCF-7 breast cancer cell line whilst complex **7** was inactive. Previous studies had indicated that complexes **3** and **6** were cytotoxic to the same cell line. Copper complexes studied by us and other, also using MCF-7 cells, had shown that these complexes had the ability to act as ROS generators and chemical nucleases therefore this study investigated whether similar behaviour was apparent for the complexes here. Complex **6** and **7** were the only complexes with DNA binding ability but neither **6** nor **7** showed any nuclease activity despite showing DNA binding properties and this is probably related to their limited ability to generate ROS. Significant ROS generation was only observed for complex **1**, and was limited for complexes **4–7** but none of the complexes showed significant nuclease activity.

Thus three of the seven complexes had shown cytotoxicity against the MCF-7 cell line which did not correlate with their ability to bind to DNA, act as a pro-oxidant or have nuclease activity, a mode of action previously ascribed to copper(II) complexes studied by our group. A number of the complexes had demonstrated ability to act as SOD and catalase mimics in cell-free assays, particularly complexes **2–4**. In contrast, in a yeast–based assay the copper complexes only had the ability to protect *S. cerevisiae* against menadione-induced oxidative stress and not hydrogen peroxide-induced stress, indicating a lack of catalase activity. The ability to act as SOD mimetics is considered to be an important therapeutic strategy given that the product of SOD is hydrogen peroxide, a pro-oxidant. In the compounds studied here though, the action of these compounds in MCF-7 cells does not appear to lead to generation of ROS in cells at a high level and will require further studies on our part to elucidate the exact mechanism of action.

Therefore the anti-cancer activity of these Schiff base complexes does not seem to be similar to other related copper complexes. Nevertheless, given the hypoxic nature of many tumours, the complexes identified here may have advantages as chemotherapeutic agents over other copper complexes identified, as their mechanism of action may not be oxidant dependent. The adaptive mechanisms in cancer cells induced by hypoxia have a selective effect on cells, with a fine-tuned protection against damage and stress, particularly against oxidative stress, thus chemotherapeutic compounds which are not pro-oxidants may offer a new therapeutic approach. Currently we are investigating the cytotoxicity of these complexes under normoxic, hypoxic and anoxic conditions to establish if their toxicity is related to oxygen concentrations in the cell.

4. Experimental details

4.1. General

All chemicals and solvents were purchased from Sigma Aldrich Ireland, Ltd., unless otherwise stated. All chemicals and solvents for the synthesis of the ligands and complexes were reagent grade and used without further purification. $CuCl_2$ stock solution was made by the dissolution of anhydrous $CuCl_2$ in water and its exact concentration was determined by complexometry through the EDTA complex. All solvents were of analytical grade and used without further purification. Doubly distilled Milli-Q water was used for sample preparation.

For the studies on wild type strain of *S. cerevisiae* cells, chemicals and solvents were purchased from Sigma Aldrich Brazil, Ltd., were of reagent grade and were used without further purification. Dehydrated media was purchased from Becton, Dickinson and Company, Brazil and were prepared in distilled water. Cultures were grown in a New Brunswick Scientific Innova®44 Incubator Shaker at 160 rpm 28 °C.

Minimum Essential Medium Eagle (Sigma Aldrich, M2279), 1% v/v L-glutamine 1% v/v (Sigma Aldrich, G7513), penicillin-streptomycin solution containing 10,000 units penicillin and streptomycin 10 mg/mL (Sigma Aldrich, F4333), 10% v/v Fetal Bovine Serum 1% v/v (Sigma Aldrich, F7524), sodium pyruvate 100 mM solution (Sigma Aldrich S8636), 1% v/v MEM Non-Essential Amino Acid solution 100× (Sigma Aldrich, M7154), T75 cm^2 tissue culture flasks (Corning, 430641 U), 3-(4,5-dimethylthiazol-2-yl)-2,5-diphenyltetrazolium bromide, (MTT) (Sigma Aldrich, M5655), cisplatinum(II) diamine dichloride (Sigma Aldrich, P4394), Poly-L-lysine (Sigma Aldrich, P4707), DMSO for molecular biology (Sigma Aldrich, D8418), Gibco MEM phenol red-free media (Biosciences, 51,200,046), Nest Biotech 96 well clear cell culture plates (Lennox Nest, APV500020), black-sided clear-bottomed 96 well plate (Corning, 3603), 2′,7′-dichlorodihydrofluorescein diacetate, H_2DCFDA, (Thermofisher Scientific, D399), tert-butyl hyperperoxide, TBHP, (Sigma Aldrich, 458,139) calf thymus DNA CT-DNA (Sigma Aldrich, D1501), 1 Kb DNA ladder (Invitrogen, 10,787–018), supercoiled pBR322 plasmid DNA (Roche, 10,481,238,001), Ultrapure Agarose, (Invitrogen, 16,500–100), Ultrapure 10× TAE buffer (Invitrogen, 15,558–026), Hepes buffer solution (Gibco, 15,630–056). $[Cu(phen)_2]^{2+}$, as $[Cu(1,10\text{-}Phen)_2](NO_3)_2$), was kindly donated by Dr. Andrew Kellet of School of Chemical Sciences and the National Institute for Cellular Biotechnology, Dublin City University, and the synthesis of which has been previously published [41].

Infrared spectra were recorded as KBr discs in the region of 4000–400 cm^{-1} on an IR Prestige-21 Shimadzu infrared spectrometer. Nuclear Magnetic Resonance (NMR) spectra were obtained using a Bruker Avance III 300 spectrometer operating at 300 MHz or Bruker Avance III 500 spectrometer operating at 500 MHz. All samples were dissolved in d_6-DMSO. Chemical shifts, δ, are given in ppm and coupling constants, J, are given in Hz. All ^{1}H NMR spectra were recorded in the region of −5 ppm to 15 ppm from TMS with a resolution of 0.18 Hz

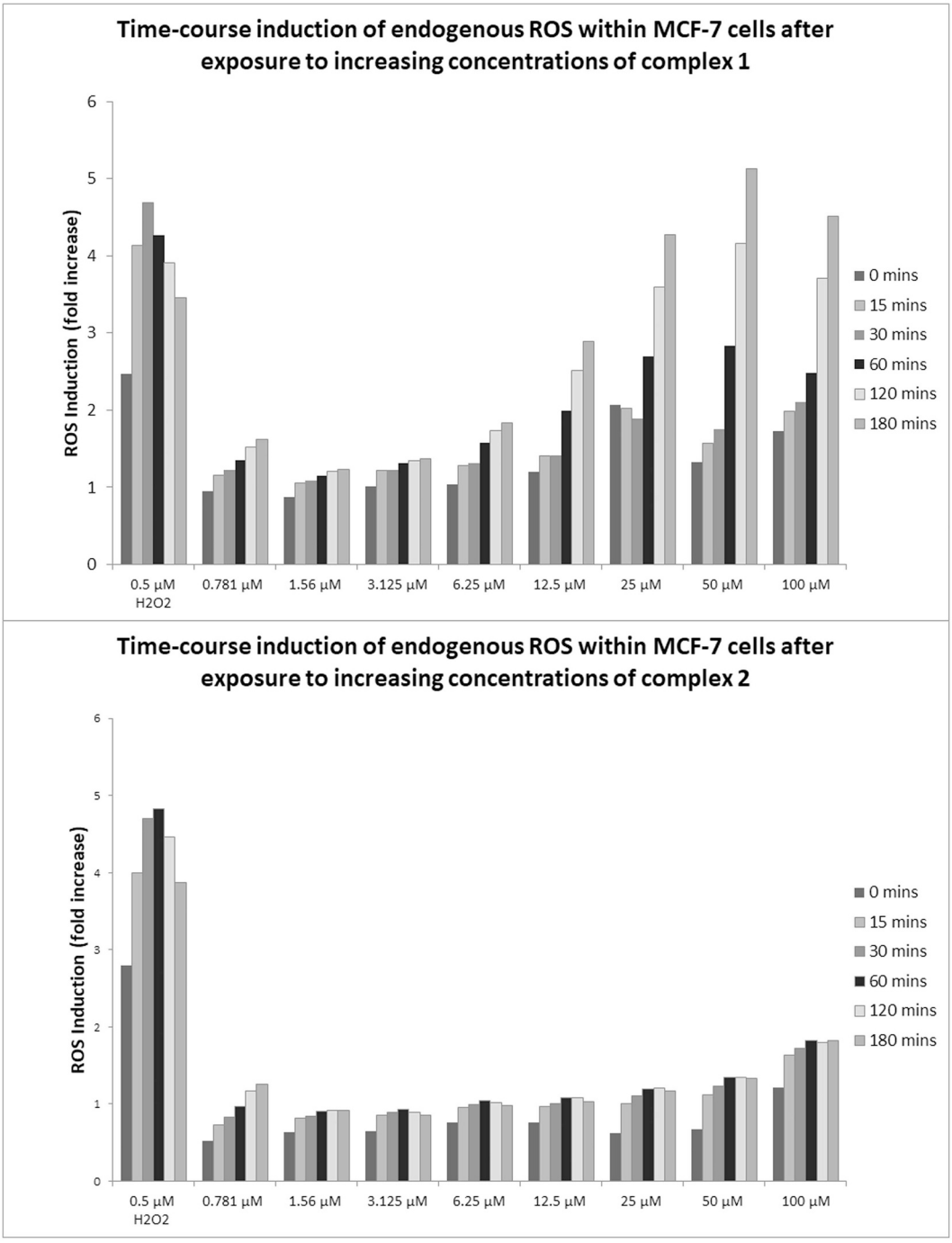

Fig. 12. Endogenous ROS induction in breast cancer cell line (MCF-7) after exposure to ROS probe 2′,7′-dichlorodihydrofluorescein diacetate and increasing concentrations of complexes **1** and **2** over a time-course of 0–180 min. (Data for remaining complexes given in Supplementary Information.)

or 0.0006 ppm. All ^{13}C NMR spectra were recorded in the region −33 ppm to 233 ppm from TMS with a resolution of 0.008 ppm. The elemental composition analyses (%CHN) were carried out in the Microanalytical Laboratory, Department of Chemistry, University College Dublin, Belfield, Dublin 4. Thermogravimetric analysis (TGA) was carried out on a Universal V4.5A TA Instrument Q50 in ITT Dublin. Melting point values were recorded on a Stuart scientific SMP1 melting point apparatus in ITT Dublin, and were taken up to a temperature of 390 °C. An Orion 710A pH-meter equipped with a Metrohm combined electrode (type 6.0234.100) and a Metrohm 665 Dosimat burette were used for the titrations. A Hewlett Packard 8452A diode array spectrophotometer was used to record the UV–vis spectra in the 200 to 950 nm window. The path length was 1 cm All EPR spectra were recorded with a BRUKER EleXsys E500 spectrometer (microwave frequency 9.81 GHz, microwave power 10 mW, modulation amplitude 5 G, modulation frequency 100 kHz). The isotropic EPR spectra were recorded at room temperature in a circulating system.

4.2. Synthesis of Coumarin-derived Schiff base ligand (L7) and copper(II) complexes (1 and 7)

The synthesis of **L1**-**L6** and complexes **2–6** were previously published, details given in Supplementary Information [20,27].

Table 6
Apparent binding DNA constants (K_{app}) of complexes **1–7** and drug controls actinomycin D and pentamidine.

Complex	Fluorescent inhibition > 50% (0–150 μM of complex)	C_{50} (μM)	K_{app} ($M(bp)^{-1}$)
Actinomycin D	Yes	9.18	1.54×10^7
Pentamidine	No	n/a	n/a
1	No	n/a	n/a
2	No	n/a	n/a
3	No	n/a	n/a
4	No	n/a	n/a
5	No	n/a	n/a
6	Yes	83.74	1.43×10^6
7	Yes	47.02	2.55×10^6

*4.2.1. Synthesis of Complex **1**: Bis[7-(3-ethoxy-2-hydroxybenzylideneamino)-4-methylcoumarin]copper(II)0.0.33 hydrate*

L1 (0.66 g, 2 mmol), was dissolved in 40 mL EtOH, to which a solution of copper(II) acetate monohydrate (0.20 g, 1 mmol) dissolved in 50 mL EtOH was added. The mixture was heated to reflux for 16 h and the brown solution was allowed to cool to room temperature. The brown precipitate was filtered off and washed with water, air dried and then dried overnight at 40 °C. Yield: 0.42 g, (58.8%); $CuC_{38}H_{3.7}N_2O_{8.3}$; 714.23 g/mol; MP 268–271 °C; IR (KBr, cm^{-1}): 1728, 1597, 1539, 1439, 1389, 1219, 1142, 1069, 858, 7410; Microanalysis found: %C 63.90%H 4.61%N 3.92, Theoretical: %C 64.45%H 4.55%N 3.96; Solubility: hot acetonitrile, DMSO; Colour: brown.

*4.2.2. Synthesis of **L7**: 7-(2,3,4-trihydroxybenzylideneamino)-4-methylcoumarin*

7-amino-4-methylcoumarin (0.70 g, 4 mmol), was dissolved in 30 mL EtOH, to which a solution of 2,3,4-trihydroxybenzaldehyde (0.63 g, 4 mmol) in 40 mL EtOH was added with a few drops of glacial acetic acid. The mixture was brought to reflux for 16 h and left to cool to room temperature. The red solution was filtered and washed with cold EtOH and left to air dry and then dried in an oven overnight at 40 °C.

Yield: 0.98 g (78.7%); $C_{17}H_{13}NO_5$; 311.29 g/mol; MP decomposes at 277 °C; IR (KBr): 3441, 1705, 1639, 1601, 1554, 1366, 1296, 1157, 1134, 1072, 858, 609, 440 cm^{-1}; Microanalysis: %C 65.14%H 4.05%N 4.31, Theoretical: %C 65.59%H 4.21%N 4.50; ^{1}H NMR (d_6-DMSO, 300 MHz, ppm, Hz): δ = 8.90 [s, 1H, H13(−CH═N−)], δ = 7.84 (d, 1H, Ar−H5, J = 8.3), δ = 7.44 (d, 1H, Ar−H8, J = 1.9), δ = 7.40 (dd, 1H, Ar−H6, J = 8.5 J = 2.0), δ = 7.02 (d, 1H, Ar−H19, J = 8.5), δ = 6.47 (d, 1H, Ar−H18, J = 8.6), δ = 6.40 [(s, 1H, H3 (vinyl)], δ = 2.45 [s, 3H, (CH3)];)]; ^{13}C NMR: C13–165.39, C2–160.38, C4, C7, C9, C15 and C17(R2) 151.61–154.49, C16(R1) – 132.88, C5–126.88, C19–125.17, C6 and C14 118.65–118.06, C3–113.75, C10–112.83, C18(R3) – 108.64, C8–108.61, C11(CH3) – 18.60; Solubility: DMSO, DMF; Colour: red.

*4.2.3. Synthesis of Complex **7**: Bis[7-(2,3,4-trihydroxybenylideneamino)-4-methylcoumarin]copper(II) trihydrate*

L7, 7-(2,3,4-trihydroxybenzylideneamino)-4-methylcoumarin (1.24 g, 4 mmol), was dissolved in 40 mL EtOH, to which was added a solution of copper(II) acetate monohydrate (0.40 g, 2 mmol) in 40 mL EtOH was added. The brown solution was brought to reflux for 16 h and left to cool to room temperature. The product was filtered and washed with cold EtOH and left to air dry and then dried in an oven overnight at 40 °C.

Yield: 0.43 g (29.1%); $CuC_{34}H_{30}N_2O_{13}$; 738.16 g/mol; IR (KBr): 3441, 1732, 1701, 1643, 1601, 1312, 1150 cm^{-1}; Microanalysis: Found: %C 54.53%H 3.26%N 3.57, Theoretical: %C 55. 32%H 4.10%N 3.80; Solubility: DMSO, DMF; Colour: brown.

4.3. Speciation studies

4.3.1. Potentiometric titrations and calculations

The pH-potentiometric measurements for the determination of the proton dissociation constants of **L1** and **L7** and the overall stability constants of the Cu(II) complexes were carried out at 25.0 ± 0.1 °C in DMSO:water 80:20 (v/v) as solvent. An ionic strength of 0.10 M (KCl) used in order to keep the activity coefficients constant. The titrations were performed with carbonate-free KOH solution of known concentration (0.10 M). The concentrations of the base and the HCl were determined by pH-potentiometric titrations. The electrode system was calibrated to the $pH = -\log[H^+]$ scale in the DMSO/water solvent mixture by means of blank titrations (strong acid vs. strong base: HCl vs. KOH), similarly to the method suggested by Irving et al. in pure aqueous solutions [42]. The average water ionization constant pK_w was 18.7 ± 0.1, which corresponds well to the literature data [27]. The reproducibility of the titration points included in the calculations was within 0.01 pH. The pH-metric titrations were performed in the pH range 2.0–15.5. The initial volume of the samples was 10.0 mL. The ligand concentration was 1 mM and metal ion-to-ligand ratios of 1:1–1:3 were used. Samples were deoxygenated by bubbling purified argon through them for approximately 10 min prior to the measurements. Argon was also passed over the solutions during the titrations. The exact concentration of the ligand stock solutions together with the proton dissociation constants were determined by pH-potentiometric titrations with the use of the computer program HYPERQUAD [43]. The same program was also utilized to establish the stoichiometry of the complexes and to calculate the stability constants ($\log\beta(M_pL_qH_r)$). $\beta((M_pL_qH_r)$ is defined for the general equilibrium $pM + qL + rH \rightleftharpoons M_pL_qH_r$ as $\beta((M_pL_qH_r) = [M_pL_qH_r] / [M]^p[L]^q[H]^r$, where M denotes the metal ion and L the completely deprotonated ligand. In all calculations exclusively titration data were used from experiments in which no precipitate was visible in the reaction mixture.

4.3.2. UV–vis spectrophotometric titrations and spectrofluorimetry

Proton dissociation constants and molar absorbance spectra of the individual ligand species were calculated using the computer program PSEQUAD [44]. The spectrophotometric titrations were performed on samples containing the ligand at 48 μM concentration in the pH range from 2 to 14.5 at 25.0 ± 0.1 °C in DMSO:water 80:20 (v/v) at an ionic strength of 0.10 M (KCl).

Three-dimensional fluorescence spectra were recorded at 250–450 nm excitations, and at 300–600 nm emission wavelengths on a Hitachi-4500 spectrofluorimeter in a 1 cm quartz cell at 25.0 ± 0.1 °C. Samples contained 0.2 μM Schiff base ligand in DMSO:water 80:20 (v/v) at 0.1 M (KCl) ionic strength.

4.3.3. EPR spectroscopic measurements and deconvolution of the spectra

The stock solution contained 1 or 2 mM ligand and 1 mM or 0.67 mM $CuCl_2$ in 80% (v/v) DMSO/H_2O at an ionic strength of 0.10 M (KCl). KOH solution was added to the stock solution to change the pH, which was measured with a Radiometer PHM240 pH/ion Meter equipped with a Metrohm 6.0234.100 glass electrode. A Heidolph Pumpdrive 5101 peristaltic pump was used to circulate the solution from the titration vessel through a capillary tube into the cavity of the instrument. The titrations were carried out under a nitrogen atmosphere. The pH range covered was 2–14.5. For several pH values 0.10 mL of sample was taken out of the stock solution and was measured individually in a Dewar containing liquid nitrogen (at 77 K).

The anisotropic spectra were analyzed individually with the EPR program [45], which gives the anisotropic EPR parameters (g_x, g_y, g_z, A_x, A_y, A_z, a_x^N, a_y^N, a_z^N), and the orientation dependent linewidth parameters (relaxation parameters α, β, γ define the linewidths through the equation $\sigma_{MI} = \alpha + \beta M_I + \gamma M_I^2$, where M_I denotes the magnetic quantum number of copper nucleus). Since a natural $CuCl_2$ was used for the measurements, the spectra were calculated as the sum of the spectra

of ^{63}Cu and ^{65}Cu weighted by their natural abundances. The copper and nitrogen coupling constants and the relaxation parameters were obtained in field units (Gauss = 10^{-4} T).

4.4. Evaluation of SOD and CAT mimetic activity using chemical assays

Procedures for both assays have been published previously and full details are given in Supplementary Information [19,46].

4.5. In vivo anti-oxidant studies

4.5.1. Evaluation of antioxidant activity in wild type BY4741 of Schiff base ligands, copper(II) complexes and copper salts

To determine SOD and CAT activity in *S. cerevisiae* wild type cells, cells were grown in 2% YPD to a concentration of 0.5–0.6 mg dry weight/cm^3 over 18–21 h in an orbital shaker at 28 °C and 160 rpm. A volume of culture with a ratio of conical flask volume/culture medium of 5/1 (either 5 or 10 mL in a 25 or 50 mL conical flask) were pre-treated with 100 μM Schiff base ligands, copper(II) complexes or copper salts for 2 h in an orbital shaker at 28 °C and 160 rpm. The cells were then exposed to a stressor, 30 mM menadione (a superoxide generator to determine SOD activity) or 2 mM hydrogen peroxide (to determine CAT activity) for 1 h in the orbital shaker.

4.5.2. Evaluation of SOD activity of selected copper(II) complexes in wild type BY4741 and sod1Δ mutant cells

To determine SOD activity exhibited by the selected complexes, BY4741 wild type and *sod1*Δ mutant cells were grown concurrently in 2% YPD to a concentration of 0.5–0.7 mg dry weight/cm^3 over 18–21 h in an orbital shaker at 28 °C and 160 rpm. A volume of culture with a ratio of conical flask volume/culture medium of 5/1 (either 5 or 10 mL in a 25 or 50 mL conical flask) were pre-treated with 100 μM of selected copper(II) complexes for 2 h in an orbital shaker at 160 rpm 28 °C. The cells were then exposed to a stressor, with wild type cells treated with 10 mM menadione and *sod1*Δ mutant cells treated with the lower concentration of 1.2 mM menadione.

4.5.3. Statistical analysis

All data displayed in the tables and graphs for the wild type cell studies were analyzed in GraphPad Prism 7 software using the statistical method one-way analysis of variance, ANOVA, at $P < 0.05$ by means of Dunnett's multiple comparisons test. ns denotes results with no statistical significance, * and ** denote statistical significance, where * indicates significant results with a P value between $> 0.01 < 0.05$ and ** denotes very significant results with a P value between $> 0.001 < 0.01$. A grey row between data indicates the complex or ligand was tested in a separate assay with its own untreated positive control (cells treated with stressor only).

4.6. Cytotoxicity assay

MCF-7 Human Breast Cancer cells were sourced from the American Tissue Culture Collection (ATCC, USA). MCF-7 cells are an adherent cell line which were grown in Minimum Essential Medium Eagle with 1% (v/v) L-glutamine, 1% (v/v) penicillin-streptomycin solution containing 10000 units penicillin and streptomycin 10 mg/mL, 10% (v/v) Fetal Bovine Serum, 1% v/v sodium pyruvate 100 mM solution and 1% (v/v) MEM Non-Essential Amino Acid solution 100×. Cells were cultured in T75 cm^2 tissue culture flasks at 37 °C in a humidified atmosphere with 5% CO_2. Cells were used between passages 6–21. Thiazolyl Blue Tetrazolium Bromide (MTT) cytotoxicity assay in MCF-7 cells was carried out according to a previously published procedure [20].

4.7. ROS assay using 2′,7′-dichlorodihydrofluorescein diacetate (H_2DCFDA) fluorescent dye

MCF-7 cells were diluted to a concentration of 1×10^5 cells per mL in MEM phenol red-free media. 100 μL of this cell suspension solution was added to microwells of a black-sided clear-bottomed 96 well plate, seeded in rows 2–12 only leaving row 1 cell free, and incubated for 24 h at 37 °C at 95% humidity and 5% CO_2. After this incubation period, media was gently removed from each microwell and washed twice with 100 μL of sterile PBS. The cells are then treated with the following solutions:

A working stock of 10 μM 2′,7′-dichlorodihydrofluorescein diacetate, DCF-DA, was prepared from a 2 mM stock solution in pure DMSO and diluted to 10 μM in PBS, giving a 0.5% v/v DMSO working stock solution. This working stock was added to 8 microwells in rows 1 and 2 and used as the diluent to prepare the 8 replicates of the positive controls. TBHP was made fresh immediately prior to plating the test solutions. 40 mM stock solutions of complex were prepared in pure DMSO and 100 μM complex or ligand solutions were prepared, giving a total of 0.5% (v/v) DMSO/PBS. 0.78 μM–100 μM of complexes were used to treat 8 replicate microwells. All microwells contained 0.5% (v/v) DMSO/PBS, (with exception to the positive control in row 3, the DMSO control), which was found to be the highest concentration of DMSO that was tolerable to the MCF-7 cells in a previous optimisation assay. Once all solutions had been added to the plate, fluorescent readings were measured on a Biotek Synergy H1 Hybrid Multi-mode Reader over 3 h at an excitation wavelength 495 nm and emission wavelength 527 nm, at a gain setting of 85 and an incubation temperature of 37 °C. The plate was returned to the incubator at a temperature of 37 °C at 95% humidity and 5% CO_2 between readings. The 8 replicates of working stock were used as a blank. This data was expressed as ROS induction as a fold increase on the negative control of cells (row 2) for each corresponding time-point. The error bars were expressed as standard error of the mean, SEM, of at least 3 independent experiments when measuring the pro-oxidant activity of the complexes and at least two independent experiments for measuring the ligands. ROS generation results are presented in graphs displayed in Supplementary Information, unless presented here. Statistical analysis was determined using the Graphpad Prism 7 package, and Dunnett's multiple comparisons test was used to determine statistical significance with significance level set at 0.05.

5. Abbreviations

CAT	catalase
CT-DNA	calf-thymus-DNA
DCF	2′,7′-dichlorofluorescein
DMF	dimethylformamide
DMSO	dimethyl sulfoxide
EDTA	Ethylenediaminetetraacetic acid
EtOH	Ethanol
H_2DCFDA	2′,7′-dichlorodihydrofluorescein diacetate
HPCINOL	1-[bis(pyridine-2-ylmethyl)amino]-3-chloro-propan-2-ol
MEM	Minimum Essential **Medium**
MTT	methylthiazolyldiphenyltetrazolium bromide
NBT	nitro blue tetrazolium
NSAIDs	non-steroidal anti-inflammatory drugs
PBS	phosphate-buffered saline
phen	phenanthroline
ROS	Reactive oxygen Species
RNS	reactive nitrogen species
SC	supercoiled
SEM	standard error of the mean
SOD	superoxide dismutase
TBHP	tert-butyl hydroperoxide
TGA	thermogravimetric analysis
YPD	Yeast Extract–Peptone–Dextrose

Acknowledgements

This work was funded by Science Foundation Ireland –Investigator Programme SFI/12/IP/1390, Technological University Dublin - Tallaght Campus President's Research Award (PRA1708) and the Centre of Applied Science for Health, *TU Dublin - Tallaght Campus, Tallaght, D24 FKT9*. This work was also supported by the National Research, Development and Innovation Office NKFIH through projects GINOP 2.3.2152016 and K115762, the J. Bolyai Research Scholarship of the Hungarian Academy of Sciences (É.A.E., N.V.M. 00383/15/7) and the UNKP 18-4 new National Excellence Program of the Ministry of Human Capacities (E.A.E) UNKP-18-4-SZTE-10. Additional support was proved under FAPERJ (Edital No. 43/2013, and Programa de Apoio ao Doutorado-Sanduíche Reverso), CNPq Edital Produtividade em Pesquisa, PQ 2011-2 and PQ 2014-0.

Appendix A. Supplementary data

Supplementary data to this article can be found online at https://doi.org/10.1016/j.jinorgbio.2019.110702.

References

[1] G. Pizzino, N. Irrera, M. Cucinotta, G. Pallio, F. Mannino, V. Arcoraci, F. Squadrito, D.A. Bitto Altavilla, Oxidative Med. Cell. Longev. 2017 (2017) 8416763.
[2] M. Schieber, N.S. Chandel, Curr. Biol. 24 (2014) 4759–4766.
[3] S. Aldosari, M. Awad, E.O. Harrington, F.W. Sellke, M.R. Abid, Antioxidants 7 (2018) 14.
[4] A.R. Phull, B. Nasir, I.U. Haq, S.J. Kim, Chem. Biol. Interact. 281 (2018) 121–136.
[5] M. Rosini, E. Simoni, A. Milelli, A. Minarini, C. Melchiorre, J. Med. Chem. 57 (2014) 2821–2831.
[6] Y. Miyata, T. Matsuo, Y. Sagara, K. Ohba, K. Ohyama, H. Sakai, Int. J. Mol. Sci. 18 (2017) 2214.
[7] M. Redza-Dtordoir, M; D.A. Averill-Bates, D.A Biochimica et Biophysica Acta (2016) 2977–2992.
[8] a C.R. Reczek, N.S. Chandel, Annu. Rev. Cancer Biol. 1 (2017) 79–98; b G. Barrera, ISRN Oncol. 2012 (2012) 1–21.
[9] A.T. Dharmaraja, J. Med. Chem. 60 (2017) 3221–3240.
[10] Y.L. Geou, S. Peter, Free Radic. Res. 44 (2010) 1–5.
[11] K. Berneis, W. Bollag, M. Kofler, H. Lüthy, Eur. J. Cancer 40 (2004) 1928–1933.
[12] M.F. Renschler, Eur. J. Cancer 40 (2004) 1934–1940.
[13] W.C. Chou, C. Jie, A.A. Kenedy, R.J. Jones, M.A. Trush, C.V. Dang, Proc. Natl. Acad. Sci. U. S. A. 101 (2004) 4578–4583.
[14] J.R. Kirshner, S. He, V. Balasubramanyam, J. Kepros, C.Y. Yang, M.Z. Du, J. Barsoum, J. Bertin, J. Mol. Cancer. Ther. 7 (2008) 2319–2327.
[15] F.P. Dwyer, E. Mayhew, E.M. Roe, A. Shulman, Br. J. Cancer 19 (1965) 195–199.
[16] R. Kachadourian, H.M. Brechbuhl, L. Ruiz-Azuara, I. Gracia-Mora, B. Day, J. Toxicology 268 (2010) 176–183.
[17] M.E. Bravo-Gómez, J.C. García-Ramos, I. Gracia-Mora, L. Ruiz-Azuara, J. Inorg. Biochem. 103 (2009) 299–309.
[18] G. Vértiz, L.E. García-Ortuño, J.P. Bernal, M.E. Bravo-Gómez, E. Lounejeva, A. Huerta, L. Ruiz-Azuara, Fundam. Clin. Pharmacol. 28 (2014) 78–87.
[19] A. Kellett, O. Howe, M. O'Connor, M. McCann, B.S. Creaven, S. McClean, A. Foltyn-Arfa Kia, A. Casey, M. Devereux, M. Free Radic, Biol. Med. 53 (2012) 564–576.
[20] B.S. Creaven, M. Devereux, D. Karcz, A. Kellett, M. McCann, A. Noble, M. Walsh, J. Inorg. Biochem. 103 (2009) 1196–1203.
[21] L. Thornton, V. Dixit, L.O.N. Assad, T. Ribeiro, D.D. Queiroz, A. Kellett, A. Casey, J. Colleran, M.D. Pereira, G. Rochford, M. McCann, D. O'Shea, R. Dempsey, S. McClean, A.F.A. Kia, M. Walsh, B.S. Creaven, O. Howe, M. Devereux, J. Inorg. Biochem. 159 (2016) 120–132.
[22] A. Kellett, M. O'Connor, M. McCann, O. Howe, A. Casey, P. McCarron, K. Kavanagh, M. McNamara, S. Kennedy, D.D. May, P.S. Skell, D. O'Shea, M. Devereux, Med. Chem. Commun. 2 (2011) 579.
[23] Z. Molphy, A. Prisecaru, C. Slator, N. Barron, M. McCann, J. Colleran, D. Chandran, N. Gathergood, A. Kellett, Inorg. Chem. 53 (2014) 5392–5404.
[24] N.Z. Yassin S.M. El-Shenawy R.F. Abdel-Rahman M. Yakoot M. Hassan S. Helmy S. Drug Des. Devel. Ther. 12 (2015) 1491–8.
[25] R. Puranik, S. Bao, A.M. Bonin, R. Kaur, J.E. Weder, L. Casbolt, T.W. Hambley, P.A. Lay, P.J. Barter, K.A. Rye, Cell Biosci 6 (2016) 9.
[26] J.E. Weder, C.T. Dillon, T.W. Hambley, B.J. Kennedy, P.A. Lay, J.R. Biffin, H.L. Regtop, N.M. Davies, Coord. Chem. Rev. 232 (2002) 95–126.
[27] B.S. Creaven, E. Czeglédi, M. Devereux, É.A. Enyedy, A. Foltyn-Arfa Kia, D. Karcz, A. Kellett, S. McClean, N.V. Nagy, A. Noble, A. Rockenbauer, T. Szabó-Plánka, M. Walsh, Dalt. Trans. 39 (2010) 10854.
[28] B.S. Creaven, M. Devereux, D. Karcz, A. Kellett, M. McCann, A. Noble, M. Walsh, J. Inorg. Biochem. 101 (2007) 1108–1119.
[29] B.S. Creaven, B. Duff, D.A. Egan, K. Kavanagh, G. Rosair, V.R. Thangella, M. Walsh, Inorganica Chim. Acta 363 (2010) 4048–4058.
[30] P. Perego, M. De Cesare, P. De Isabella, N. Carenini, G. Beggiolin, G. Pezzoni, M. Palumbo, L. Tartaglia, G. Pratesi, C. Pisano, P. Carminati, G.L. Scheffer, F. Zunino, Cancer Res. 61 (2001) 6034–6603.
[31] A.G. Gutiérrez, A. Vázquez-Aguirre, J.C. García-Ramos, M. Flores-Alamo, E. Hernández-Lemus, L. Ruiz-Azuara, C. Mejía, J. Inorg. Biochem. 126 (2013) 17–25.
[32] M. Devereux, D. O'Shea, A. Kellett, M. McCann, M. Walsh, D. Egan, C. Deegan, K. Kedziora, G. Rosair, H. Müller-Bunz, J. Inorg. Biochem. 101 (2007) 881–892.
[33] A. Horn, G.L. Parrilha, K.V. Melo, C. Fernandes, M. Horner, L.D.C. Visentin, J.A.S. Santos, M.S. Santos, E.C.A. Eleutherio, M.D. Pereira, Inorg. Chem. 49 (2010) 1274–1276.
[34] T.P. Ribeiro, C. Fernandes, K.V. Melo, S.S. Ferreira, J.A. Lessa, R.W.A. Franco, G. Schenk, M.D. Pereira, A. Horn, Free Radic. Biol. Med. 80 (2015) 67–76.
[35] D.J. Jamieson, Yeast 14 (1998) 1511–1527.
[36] K. Mišković, M. Bujak, M. Baus Lončar, L. Glavaš-Obrovac, Arch. Ind. Hyg. Toxicol. 64 (2013) 593–602.
[37] C. Pérez-Arnaiz, N. Busto, J.M. Leal, B. García, J. Phys. Chem. B 118 (2014) 1288–1295.
[38] C. Slator, N. Barron, O. Howe, A. Kellett, ACS Chem. Biol. 11 (2016) 159–171.
[39] M. O'Connor, A. Kellett, M. McCann, G. Rosair, M. McNamara, O. Howe, B.S. Creaven, S. McClean, A.F.A. Kia, D. O'Shea, M. Devereux, J. Med. Chem. 55 (2012) 1957–1968.
[40] A. Kellett, M. O'Connor, M. McCann, M. McNamara, P. Lynch, G. Rosair, V. McKee, B.S. Creaven, M. Walsh, S. McClean, A. Foltyn-Arfa Kia, D. O'Shea, O. Howe, M. Devereux, Dalton Trans. 40 (2011) 1024–1027.
[41] A. Prisecaru, V. McKee, O. Howe, G. Rochford, M. McCann, J. Colleran, M. Pour, N. Barron, N. Gathergood, A. Kellett, J. Med. Chem. 56 (2013) 8599–8615.
[42] H.M. Irving, M.G. Miles, L.D. Pettit, Anal. Chim. Acta 38 (1967) 475–488.
[43] P. Gans, A. Sabatini, A. Vacca, Talanta 43 (1996) 1739–1753.
[44] L. Zékány, I. Nagypál, D.L. Leggett (Ed.), Computational Methods for the Determination of Stability Constants, Plenum Press, New York, 1985, p. 291.
[45] A. Rockenbauer, L. Korecz, Appl. Magn. Reson. 10 (1996) 29–43.
[46] M. Mujahid, A. Foltyn-Arfa Kia, B. Duff, D.A. Egan, M. Devereux, S. McClean, M. Walsh, N. Trendafilova, I. Georgieva, B.S. Creaven, J. Inorg. Biochem. 153 (2015) 103–113.